

# Creep and Tensile Properties of Several Oxide Dispersion Strengthened Nickel Base Alloys

J. DANIEL WHITTENBERGER

The room temperature and 1365 K tensile properties and 1365 K tensile creep properties at low strain rates were measured for several oxide dispersion strengthened (ODS) alloys. The alloys examined included ODS Ni, ODS Ni-20Cr and ODS Ni-16Cr-4/5Al. Metallography of creep tested, large grain size ODS alloys indicated that creep of these alloys is an inhomogeneous process. All alloys appear to possess a threshold stress for creep. It is believed that the threshold stress is associated with diffusional creep in the large grain size ODS alloys and normal dislocation motion in perfect single crystalline ODS alloys. Threshold stresses for large grain size ODS Ni-20Cr and Ni-16Cr-4/5Al type alloys are dependent on the grain aspect ratio. Because of the deleterious effect of prior creep on room temperature mechanical properties of large grain size ODS alloys, it is speculated that the threshold stress may be the design-limiting creep strength property.

**O**XIDE dispersion strengthened (ODS) nickel-base alloys have potential for use in rather demanding elevated temperature environments, such as aircraft turbine engines. The first generation of commercial ODS Ni alloys, nominally Ni-2ThO<sub>2</sub>, exhibited excellent strength in the temperature range 1255 to 1475 K and over temperature capacity almost up to the melting point.<sup>1,2</sup> Unfortunately the Ni-2ThO<sub>2</sub> alloys were subject to severe oxidation attack.<sup>3</sup> For improved oxidation resistance, the Ni-20Cr-2ThO<sub>2</sub> type alloys were developed. These alloys possess good elevated temperature strength and over temperature capacity<sup>4,5</sup> plus excellent static oxidation resistance;<sup>6</sup> however, the dynamic oxidation resistance at  $T \gtrsim 1255$  K was low due to the volatilization of chromium oxide.<sup>7,8</sup> Most recently, Ni-16Cr-Al (nominally 4 to 6 wt pct) type ODS alloys have been developed.<sup>9,10</sup> These alloys form an Al<sub>2</sub>O<sub>3</sub> protective oxide scale and possess dynamic oxidation resistance as well as other desirable properties.<sup>10,11</sup> Ni-16Cr-Al alloys containing either thoria or yttria as the dispersoid have been produced; a yttria strengthened alloy is especially attractive as it eliminates the radioactivity problems associated with thoriated alloys.

The high temperature strength of ODS alloys is due to the presence of a uniform dispersion of fine, inert particles.<sup>12</sup> The particles produce direct strengthening by acting as dislocation barriers, and in polycrystalline ODS alloys the particles affect the grain size and grain shape which also influences the mechanical properties.<sup>12</sup> In general, only an elongated grain structure is required for strength parallel to the direction of primary working; however, a large grain size, semi-elongated microstructure is probably necessary for reasonable transverse properties.<sup>13</sup> Most theories of strengthening in ODS alloys have considered the consequences of the direct strengthening effect involving interactions between the dispersoid particles and dislocations.<sup>12</sup> However, in creep type applications, deformation mechanisms

involving the grain structure may be more important. For example, recent work by Kane and Ebert<sup>14</sup> estimated that creep at 1365 K in polycrystalline TD-NiCr (Ni-20Cr-2ThO<sub>2</sub>) is entirely due to diffusion controlled grain boundary sliding, *i.e.*, diffusional creep.<sup>15</sup> Some microstructural evidence<sup>16,17</sup> of diffusional creep exists for several polycrystalline ODS alloys. In addition, several investigations of ODS alloys have presented data which suggests that creep is not a homogeneous process and that a threshold stress for creep (stress below which creep does not occur) exists.<sup>16,19</sup>

This work was undertaken to study the creep behavior at 1365 K of typical ODS Ni, Ni-20Cr, and Ni-16Cr-4Al alloys. In general, creep exposures involved low strains, on the order of 1 pct or less, after nominally 100 h of testing. Particular attention was directed toward assessment of threshold stress for creep and examination of microstructures for evidence of diffusional creep and inhomogeneity of creep. In addition, short term tensile properties at room temperature and 1365 K were determined.

## EXPERIMENTAL PROCEDURE

The nominal chemistry of the ODS alloys evaluated is shown in Table I. Two alloys were produced by Fansteel, Inc.: TD-Ni in the form of heat treated (stress relieved) 1.27 cm diam bar, and TD-NiCrAl as a steel canned 20 cm diam extrusion billet. DS-

Table I. Nominal Alloy Chemistry, Wt Pct

Alloy	Cr	Al	C	ThO <sub>2</sub>	Y <sub>2</sub> O <sub>3</sub>	Ni
TD-Ni (heat 3062)	—	—	0.027	2	—	Balance
DS-NiCr	20.3	—	0.009	2	—	Balance
Inconel MA-754* (heat OT0055B)	20	0.6	0.07	—	0.6	Balance
TD-NiCrAl (heat 3939)	16	4.2	0.05	2	—	Balance
DST-NiCrAl	16	5	0.013	2	—	Balance

\*Also contains 1.5 Fe and 1.0 Ti

J. DANIEL WHITTENBERGER is Materials Engineer, NASA Lewis Research Center, Cleveland, OH 44135.

Manuscript submitted November 4, 1976.

NiCr was obtained from Stellite Division-Cabot Corporation in the form of unrecrystallized, 1.9 × 6.4 cm sheet bar. Inconel MA-754 was produced by Huntington Alloy, Inc. in the form of heat treated 2.8 × 8.3 cm sheet bar. The experimental alloy DST-NiCrAl was obtained from Sherritt-Gordon Mines, Ltd. in the form of pressed and sintered billets with a nominal diam of 7.6 cm.

Unrecrystallized DS-NiCr was heat treated before testing. The alloys in billet form were subjected to various thermomechanical processing and heat treatment schedules in order to obtain an elongated microstructure with a uniform large grain size. The final processing and heat treatment schedules for all of the ODS alloys are shown in Table II. The average grain size parameters determined by linear analysis and the crystallographic texture of the alloys are given in Table III. Dispersoid particle sizes or inter-particle spacings were not determined for these alloys.

Round bar tensile type specimens with a nominally 2.8 cm long × 0.51 cm diam gage section were centerless ground from the heat treated alloys. In general,

tapered grip end specimens were used; however, threaded grip end specimens were used for DS-NiCr tested in the long transverse direction and for Inconel MA-754 in order to conserve material. All alloys were tested parallel to the extrusion axis. In addition, DS-NiCr and Inconel MA-754 were tested in the long transverse direction (long axis of cross section of bar).

All creep testing was conducted in accordance with ASTM specifications at 1365 K in air on constant load test machines. Creep tests were generally designed to produce between 0.1 and 1 pct strain in 100 h; however, a few specimens were tested to rupture. Elongation as a function of time was measured optically from scribed platinum strips which had been spot welded to the shoulders of the test specimens. As creep testing was generally confined to low strain rates ( $<5 \times 10^{-8} \text{ s}^{-1}$ ), it should be noted that the precision of the strain measurements is on the order of 0.0002. Thus the creep strains and creep rates are subject to measurement errors which can introduce scatter into the data. Testing was interrupted for many specimens after 100 to 150 h; these specimens were then subjected to tensile testing to determine the effect of prior creep. The results of residual tensile testing are described elsewhere.<sup>20</sup>

In addition to creep tests, tensile tests were conducted at room temperature and 1365 K. Room temperature testing was conducted on an oil hydraulic test machine at a cross head speed of about 0.001 cm/s with strain through the 0.2 pct yield measured by a clip-on extensometer. Tensile testing at 1365 K was conducted at a constant cross head speed of 0.002 cm/s and the 0.2 pct yield stress was estimated from load-cross head motion plots. Selected tensile and rupture tested specimens were subjected to metallographic examination.

Table II. Thermal-Mechanical Processing and Heat Treatment Schedules

Alloy	Thermal Mechanical Processing	Heat Treatment
TD-Ni	Not reported by vendor	Not reported by vendor
DS-NiCr	Extruded ~12 l at ~1365 K by vendor	Heated from 1475 to 1590 K in 2 h
Inconel MA-754	Not reported by vendor	Not reported by vendor
TD-NiCrAl	Extruded 12 l at 1365 K to 3 × 10 cm sheet bar, hot rolled to 1.5 cm thickness in two 30 pct passes at 1365 K	2 h at 1640 K
DST-NiCrAl	Canned in steel, extruded 16:l at 1395 K to ~1.7 cm diam bar	2 h at 1640 K

Table III. Grain Size Parameters and Texture of ODS Alloys

(a) Grain Size					
Alloy	Characteristic Lengths, $\mu\text{m}$			Average Grain Size, $\mu\text{m}$ $0.85 \sqrt[3]{L_1 L_2 L_3}$	Gram Aspect Ratio, $\text{GAR} = L_1 / \sqrt{L_2 L_3}$ $(\sqrt{L_2 L_3} / L_1)^*$
	Parallel to Extrusion Axis, $L_1$	Long Transverse, $L_2$	Short Transverse, $L_3$		
TD-Ni	25		1.3 diam	3.5	19
DS-NiCr	Single crystal with very large elongated low angle grains approximately 1 cm diameter by 10 cm length. Low angle grains elongated along extrusion axis.			—	—
Inconel MA-754	530	180	115	250	3.68 (0.73)
TD-NiCrAl	490	285	150	235	2.37
DST-NiCrAl	1200	300 diam (duplex: 660 and 120 $\mu\text{m}$ diameter)		400	1.82†
(b) Texture					
Alloy	Orientation				
TD-Ni	Wire, [100] parallel to extrusion axis				
DS-NiCr	[100] parallel to extrusion axis [011] parallel to long transverse direction [0 $\bar{1}$ 1] parallel to short transverse direction				
Inconel MA-754	Same as DS-NiCr				
TD-NiCrAl	Same as DS-NiCr				
DST-NiCrAl	Wire, [522] parallel to extrusion axis				

\*Calculated for transverse testing.

†Calculated for larger grain diameter.

## RESULTS AND DISCUSSION

### Tensile Properties

The room temperature and 1365 K tensile properties of the ODS alloy are shown in Table IV. At room temperature the Ni-16Cr-Al type alloys are considerably stronger than the Ni or Ni-20Cr types; this strength is probably due to the presence of  $\gamma'$  and solid solution hardening effects of Al. Previous work<sup>9,10</sup> has shown that Ni-16Cr alloys with more than about 3.5 Al contain  $\gamma'$ . The higher strength of Inconel MA-754 in comparison to DS-NiCr is probably due to the combined solid solution hardening effects of Al and Ti. Both Inconel MA-754 and DS-NiCr are stronger parallel to the extrusion axis ([100] direction) than in the long transverse direction ([011] direction). This is probably due to slip on multiple slip systems leading to strain hardening for the [100] direction, while only one slip system is operating in [011] direction.

At room temperature all the alloys exhibited reasonable tensile elongations, and all failures were intragranular. DS-NiCr tested in the long transverse direction exhibited multiple necks which lead to the very high tensile elongation. Only DS-NiCr tested in the long transverse direction exhibited multiple necking.

With the exception of Inconel MA-754, all of the alloys possessed similar tensile strengths at 1365 K;

Inconel MA-754 is considerably stronger. DS-NiCr and TD-NiCrAl were very ductile, and the fractures were intragranular. Inconel MA-754 and DST-NiCrAl tested parallel to the extension axis exhibited reasonable ductility; however, the fractures were intergranular with grain boundary cracking evident in the microstructures. Inconel MA-754 tested in the long transverse direction exhibited low ductility, and the fracture was intergranular. TD-Ni possessed moderate ductility and the fracture was probably intergranular.

The tensile test data in Table IV for TD-Ni, DS-NiCr, and TD-NiCrAl agree well with that determined by other investigators.<sup>1,9,21</sup>

Comparison of the 1365 K tensile strength data in Table IV with the grain size parameter in Table III reveals that no correlation exists between strength and grain size. There does, however, seem to be a linear relationship, as suggested by Wilcox and Clauer,<sup>12</sup> between 1365 K tensile strength properties and grain aspect ratio for large grain size ODS alloys tested parallel to the extrusion axis. This relationship is shown in Fig. 1; it should be noted that the one example of a low grain aspect ratio material (Inconel MA-754: transverse) does not follow the commonly held concept of low grain aspect ratio being equivalent to low strength. Additionally, the strength of TD-Ni is not predictable by extrapolation of the curve in Fig. 1. This is probably a result of the

Table IV. Tensile Properties of Several ODS Alloys

Alloy	Test Direction	Tensile Properties				
		0.02 Pct Yield, MPa	0.2 Pct Yield, MPa	UTS, MPa	Elongation, Pct	RA, Pct
Room Temperature						
TD-Ni	Parallel to ext. axis	440	469	482	20	79
		350	418	493	19	82
		373	435	490	19	78
DS-NiCr	Parallel to ext. axis	373	398	803	22	28
		352	380	789	26	36
DS-NiCr	Long transverse	—	442	626	42	43
Inconel MA-754	Parallel to ext. axis	626	688	1052	23	21
		589	646	1021	20	23
Inconel MA-754	Long transverse	581	655	932	23	29
		571	657	937	23	27
TD-NiCrAl	Parallel to ext. axis	730	786	1179	11	10
DST-NiCrAl	Parallel to ext. axis	675	746	1062	16	14
		677	777	1128	15	16
		692	720	1073	13.6	14
1365 K						
TD-Ni	Parallel to ext. axis	—	104	119	3.6	6
		—	99	112	4.5	6
		—	93	120	3.6	6
DS-NiCr	Parallel to ext. axis	—	94	107	17	69
		—	97	106	19	52
DS-NiCr	Long transverse	—	—	Not measured	—	—
Inconel MA-754	Parallel to ext. axis	—	148	151	9.5	12
		—	149	152	9.5	11.3
Inconel MA-754	Long transverse	—	154	154	2.6	1.5
		—	154	154	2.5	1.6
TD-NiCrAl	Parallel to ext. axis	—	102	108	21	45
		—	99	105	19	44
DST-NiCrAl	Parallel to ext. axis	—	90	103	12	15
		—	83	92	7	11
		—	81	92	13.6	13

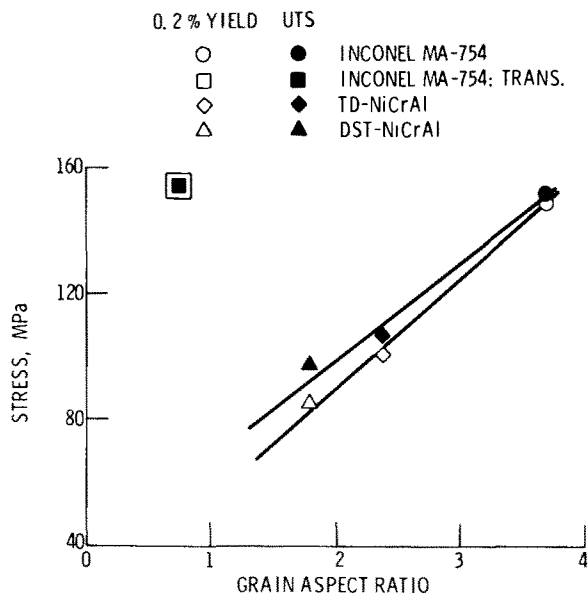


Fig. 1--1365 K tensile strength properties of several large grain size ODS alloys as a function of grain aspect ratio.

small grain size of TD-Ni and the previously observed behavior<sup>12</sup> that ODS Ni alloys are weaker than ODS Ni base alloys.

### Creep Behavior

**Creep Data and Analysis.** Table V contains the creep data tabulated for all the alloy-direction combinations evaluated in this study. Data are presented for strains at 1 h to indicate the amount of transient creep; in general, the alloys were in steady state creep after 1 h of testing. With the exception of DS-NiCr, the alloys were generally in third stage creep after about 0.5 pct strain. DS-NiCr tested parallel to the extrusion axis did not enter third stage creep until about 2 pct strain. DS-NiCr tested in the long transverse direction appeared to undergo very little deformation prior to failure; however, from the elongation and reduction in area measurements from the failed specimens, considerable deformation occurred in a short time during the rupture process. Because of this and the scatter in the creep-rupture data in

Table V. Creep and Creep Rupture Properties of Several ODS Alloys at 1365 K

Specimen	Stress, MPa	Time, h	Strain, Pct		Steady State Creep Rate, s <sup>-1</sup>	Comments
			1 h	End Test		
TD-Ni Parallel to Extrusion Axis						
N-1*	75.8	91.1 (failed)	0.21	~2.5	1.3 × 10 <sup>-8</sup>	0.65 pct strain at 79.1 h
N-6*	68.9	43.3 (failed)	0.4	~2	1.45 × 10 <sup>-8</sup>	0.74 pct strain at 43.25 h
N-50	65.5	142.4	0.27	0.49	2.35 × 10 <sup>-9</sup>	
N-53	62.0	120.5	0.12	0.35	Ill defined curve	
N-52	58.6	141.0	0.16	0.30	1.6 × 10 <sup>-9</sup>	
N-56	55.1	148.4	0.05	0.20	<10 <sup>-9</sup>	
N-5*	55.1	116.9	0.14	0.18	<10 <sup>-9</sup>	Curve flat after 1 h
N-10	48.2	117.3	0.19	0.25	<10 <sup>-9</sup>	Curve flat after 20 h
N-4*	48.2	120.5	0.02	0.12	<10 <sup>-9</sup>	Curve flat after 20 h
Inconel MA-754. Parallel to Extrusion Axis						
L-16	89.6	73.1	0.2	1.0	2.5 × 10 <sup>-8</sup>	
L-13	86.1	82.5	0.15	~0.5	1.2 × 10 <sup>-8</sup>	0.48 pct at 74.7 h pulled out grip 82.5 h
L-2	82.7	100.1 (failed)	0.1	~3.5	1 × 10 <sup>-8</sup>	0.72 pct at 88.7 h
L-5	82.7	100.4	0.1	0.435	1.1 × 10 <sup>-8</sup>	
L-12	82.7	69.0	0.15	~0.3	7 × 10 <sup>-9</sup>	0.27 pct at 50.5 h pulled out grip 69.0 h
L-4	82.7	67.8 (failed)	0.08	~3.5	2.5 × 10 <sup>-8</sup>	1.10 pct at 67.2 h
L-7	75.9	141.1	0.05	0.313	4.3 × 10 <sup>-9</sup>	
L-15	75.9	47.8	0.12	~0.22	4.9 × 10 <sup>-9</sup>	0.17 pct at 20.5 h pulled out grip 47.8 h
L-14	72.3	141.9	0.10	0.11	<10 <sup>-9</sup>	Curve flat after 1 h
L-8	68.9	141.6	0.08	0.1	<10 <sup>-9</sup>	Curve flat after 1 h
L-3	65.5	145.1	0.05	0.12	<10 <sup>-9</sup>	Curve flat after 20 h
Inconel MA-754 Parallel to Long Transverse Direction						
T-7	34.5	67.3	0.08	1.67	3.8 × 10 <sup>-8</sup>	
T-6	27.6	72.7	0.15	1.24	3.35 × 10 <sup>-8</sup>	
T-1	24.1	101.0	0.04	0.91	1.1 × 10 <sup>-8</sup>	
T-13	22.4	94.1	0.11	~0.22	3.35 × 10 <sup>-9</sup>	0.22 pct at 90.8 h power failure 94.1 h
T-3	20.7	120.3	0	0.49	1.3 × 10 <sup>-8</sup>	
T-11	20.7	149.2	0	0.06	1 × 10 <sup>-9</sup>	
T-2	18.9	148.7	0.03	0.44	4.45 × 10 <sup>-9</sup>	
T-14	17.2	149.5	0.02	0.12	<10 <sup>-9</sup>	Curve flat after ~50 h
T-5	13.8	148.3	0.05	0	<10 <sup>-9</sup>	Curve flat

(continued)

Table V (Continued)

Specimen	Stress, MPa	Time, h	Strain, Pct		Steady State Creep Rate, s <sup>-1</sup>	Comments
			1 h	End Test		
DS-NiCr Parallel to Extrusion Axis						
S-11	86.1	3.05 (failed)	2.2	17.3 (61 pct RA)	4.4 × 10 <sup>-6</sup>	5.04 pct at 2.4 h
S-15	82.1	11.9 (failed)	0.085	17.3 (60 pct RA)	8.6 × 10 <sup>-7</sup>	2.97 pct at 7.25 h
S-3	79.2	98.3	0.5	1.64	2.6 × 10 <sup>-8</sup>	
S-5	75.9	115.1	0	0.6	1.1 × 10 <sup>-8</sup>	
S-9	72.3	101.4	0	0.3	7.6 × 10 <sup>-9</sup>	
S-8	68.9	500	0.2	0.2	<10 <sup>-9</sup>	Curve flat after 1 h
S-12	68.9	115.7	0.03	0.08	<10 <sup>-9</sup>	
S-13	65.5	101.0	0.03	0.18	4 × 10 <sup>-9</sup>	
S-14	62.0	119.5	0.02	0.13	<10 <sup>-9</sup>	Curve flat after 7 h
DS-NiCr Parallel to Long Transverse Direction						
ST-11	82.7	88.6	0.07	0.32	5.2 × 10 <sup>-9</sup>	
ST-12	79.2	31.5 (failed)	0.02	5.4 (13 pct RA)	<10 <sup>-9</sup>	0.11 pct at 31.4 h Curve flat after 3.5 h
ST-6	79.2	17.3 (failed)	0.1	5.7 (6.2 pct RA)	—	0.16 pct at 5.7 h
ST-1	75.9	113.7 (failed)	0.04	3.8 (9.3 pct RA)	<10 <sup>-9</sup>	0.08 pct at 104.2 h Curve flat after 3.5 h
ST-8	75.9	0.5 (failed)	—	3 (3.5 pct RA)	—	0.03 pct at 0.4 h
ST-9	68.9	146.2	0.01	0.1	1.5 × 10 <sup>-9</sup>	
ST-7	62.0	150.3	0.06	0.15	2 × 10 <sup>-9</sup>	
ST-4	27.6	147.9	0.03	0.03	<10 <sup>-9</sup>	Curve flat after 1 h
Load increased to ST-5	55.1 24.1	146.7 141.1	0.03 0	0.07 0	<10 <sup>-9</sup> <10 <sup>-9</sup>	Curve flat after 10 h Curve flat
Load increased to ST-3	48.2 34.5	135.3 148.6	0.01 0	0.03 0	<10 <sup>-9</sup> <10 <sup>-9</sup>	Curve flat after 5 h Curve flat
ST-2	31.0	150.3	0	0	<10 <sup>-9</sup>	Curve flat
TD-NiCrAl Parallel to Extrusion Axis						
TL-5	75.8	39.5 (failed)	0.2	7.0	—	2.4 pct at 28.6 h
TL-4	68.9	<46.9 (failed)	0.2	5.4	1 × 10 <sup>-7</sup>	1 pct at 23.1 h
TL-11	62.0	90.0 (failed)	0.1	Multiple fracture	1.9 × 10 <sup>-8</sup>	0.94 pct at 68.6 h
TL-9	55.1	74.8	0.07	1.8	2.6 × 10 <sup>-8</sup>	
TL-7	55.1	44.0	0.15	0.57	2.35 × 10 <sup>-8</sup>	
TL-12	51.7	115.7	0.1	0.11	<10 <sup>-9</sup>	Curve flat after 1 h
TL-10	48.2	118.0	0.05	0.12	<10 <sup>-9</sup>	Curve flat after 5 h
TL-6	44.8	115.8	0.05	0.05	<10 <sup>-9</sup>	Curve flat after 1 h
TL-8	41.3	114.2	0.02	0.1	<10 <sup>-9</sup>	
DST-NiCrAl Parallel to Extrusion Axis						
T-8-8	62.0	102.0	0.55	3.46	—	Steady-state region not defined
T-8-6	55.1	142.2	0.08	0.68	7.3 × 10 <sup>-9</sup>	
T-9-3	55.1	137.9	0.01	0.51	1.65 × 10 <sup>-8</sup>	Essentially no creep first 50 h
T-9-2	51.7	163.9	0.15	0.3	3.40 × 10 <sup>-9</sup>	
T-9-4	48.2	118.9	0	0.19	2.85 × 10 <sup>-9</sup>	
T-8-7	48.2	140.3	0.05	0.28	4.2 × 10 <sup>-9</sup>	
T-8-12	44.8	168.0	0.11	~0.3	1.75 × 10 <sup>-9</sup>	
T-9-7	44.8	165.8	0.05	0.25	1.85 × 10 <sup>-9</sup>	
T-8-4	41.3	148.9	0.08	0.24	<10 <sup>-9</sup>	Curve flat after 75 h
T-9-5	41.3	147.8	0	0	<10 <sup>-9</sup>	Curve flat
T-8-3	41.3	150.1	0	0.18	2.4 × 10 <sup>-9</sup>	
T-9-6	41.3	146.8	0.03	0.27	3.7 × 10 <sup>-9</sup>	

\*Plasma coated with Ni-20Cr, approximately 100 μm thick.

Table V, the creep behavior of DS-NiCr in the long transverse direction could not be characterized. In this study creep rates less than 10<sup>-9</sup> s<sup>-1</sup> could not be determined as they were below the limit of detection.

Even with the previously mentioned difficulties in measuring small amount of creep, most of the alloys exhibited the usual empirical creep rate rela-

tionship for stress dependency at strain rates greater than about 2 × 10<sup>-9</sup> s<sup>-1</sup> as follows:

$$\dot{\epsilon} \propto \sigma^\eta \quad [1]$$

where  $\dot{\epsilon}$  is the strain rate,  $\sigma$  is the applied tensile stress, and  $\eta$  is the stress exponent. The only alloy which did not follow Eq. [1] was DS-NiCr tested in

the long transverse direction. Typical examples of power law behavior are presented in Fig. 2. All stress exponents for the alloys are listed in Table VI: in general, the power law exponents are high which is apparently normal for most ODS alloys.<sup>18</sup>

All of these alloy systems appear to possess a "threshold" stress below which creep does not occur. Approximate threshold stresses are given in Table VI. These were estimated from the strain rate data and shape of strain-time curves from Table V and residual tensile property data.<sup>20</sup> In general, creep exposures at or slightly below the threshold stress did produce a small amount (~0.1 pct) of transient creep. Once transient creep was finished, however, test specimens exhibited little, if any, further deformation over extended periods of time. (For example, specimens N-10, L-14, T-5, S-8 ST-4, TL-12, and T-9-5.) The strain rate data were also fitted to a modified power law stress dependency equation:

$$\dot{\epsilon} \propto (\sigma - \sigma_0)^{n'} \quad [2]$$

where  $\sigma_0$  is the estimated threshold stress for creep from Table IV and  $n'$  is the effective stress exponent. The effective stress exponents are also presented in Table IV. Figure 2 also illustrates a typical example of the modified power law behavior. In general, the fit of the strain rate data for the polycrystalline alloys is fair, at best. However, all these alloys possessed low (<3) effective stress exponents which suggests that diffusional creep is a possible mechanism.

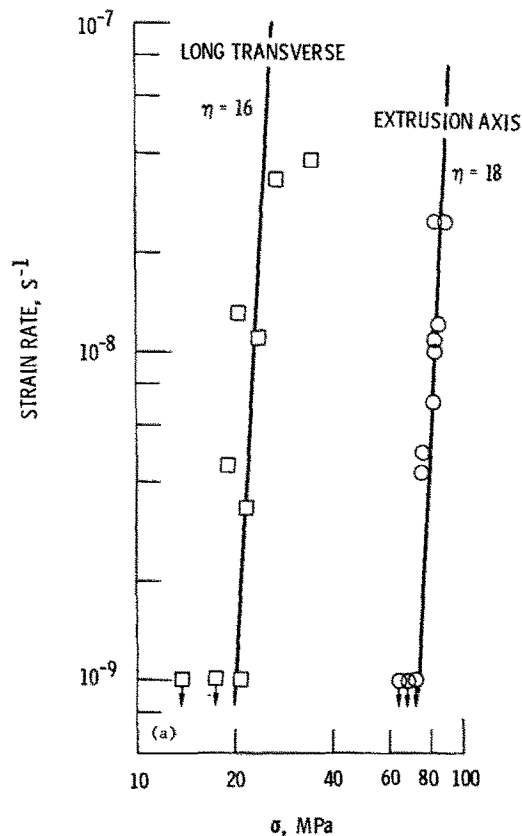


Fig. 2—Steady state creep rate of Inconel MA-754 as a function of (a) applied stress ( $\sigma$ ) for testing in the extrusion direction and long transverse direction, (b) effective stress ( $\sigma - \sigma_0$ ) for testing in extrusion direction, and (c) effective stress ( $\sigma - \sigma_0$ ) for testing in long transverse direction.

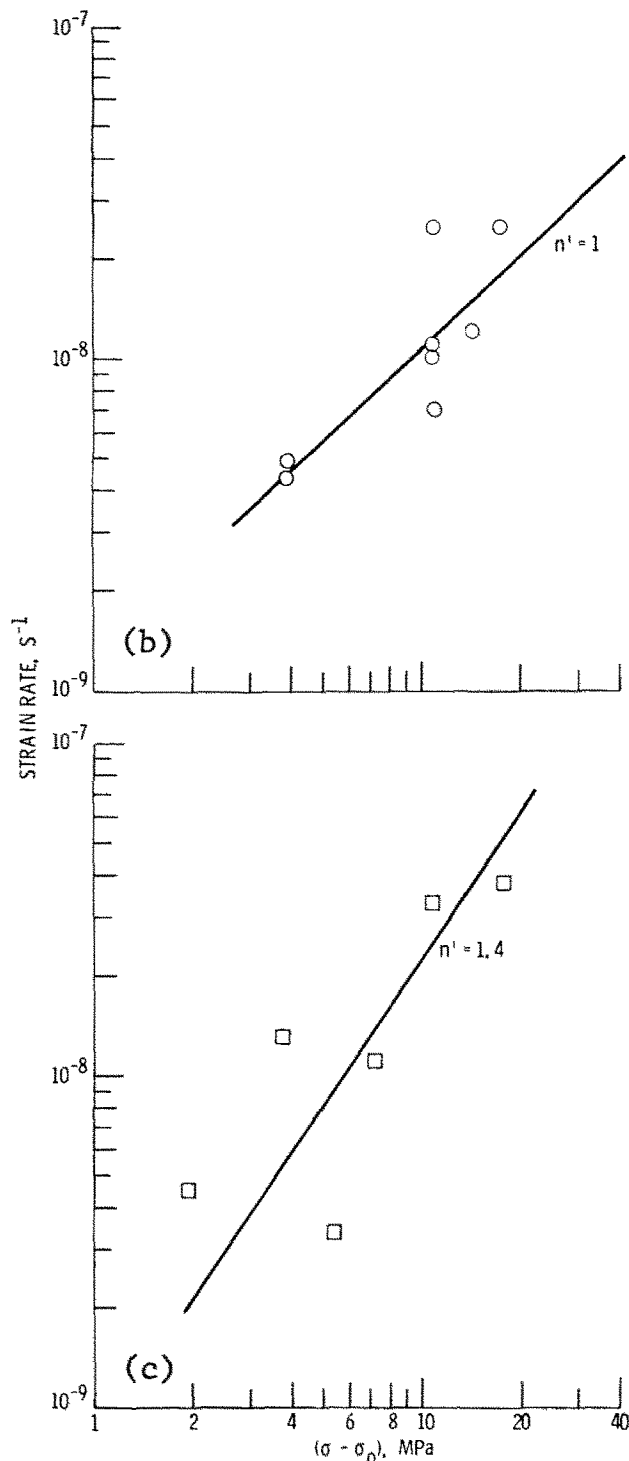


Fig. 2—Continued.

The creep rate of DS-NiCr tested parallel to the extrusion axis was well described by Eq. [2] for  $\dot{\epsilon} > 10^{-8} \text{ s}^{-1}$  where the effective stress exponent was about nine. An effective stress exponent of nine is in agreement with Lin and Sherby's analysis<sup>19</sup> of Lund and Nix's creep data<sup>18</sup> for single crystalline Ni-20Cr-2ThO<sub>2</sub> (TD-NiCr).

**Metallography.** Rupture tested TD-Ni possessed a few cavities in the vicinity of the fracture and DS-NiCr tested parallel to the extrusion axis to rupture contained a few small cracks within the necked region and on the surface of the necked region. The micro-

structure of the interrupted creep test specimens after room temperature tensile testing was identical to the as-received (untested) microstructure for these two alloy-direction combinations.<sup>20</sup>

Metallography of the failed specimens of Inconel MA-754 and TD-NiCrAl tested parallel to the extrusion axis and DS-NiCr tested in the long transverse direction revealed that the fractures were intergranular and evidence for diffusional creep exists. Such evidence consisted of dispersoid-free bands, intergranular cavitation and/or cracking, and internal oxidation at or near grain boundaries. Typical examples of dispersoid-free bands and cracking coupled with internal oxidation are shown in Fig. 3. Similar microstructural features were seen in creep and rupture tested TD-NiCr (Ref. 16) and in many interrupted creep test specimens of Inconel MA-754, TD-NiCrAl, and DST-NiCrAl after tensile testing at room temperature.<sup>20</sup>

While such features are clearly visible in the gage sections of test specimens which experienced as little as 0.2 to 0.3 pct creep strain, these microstructural

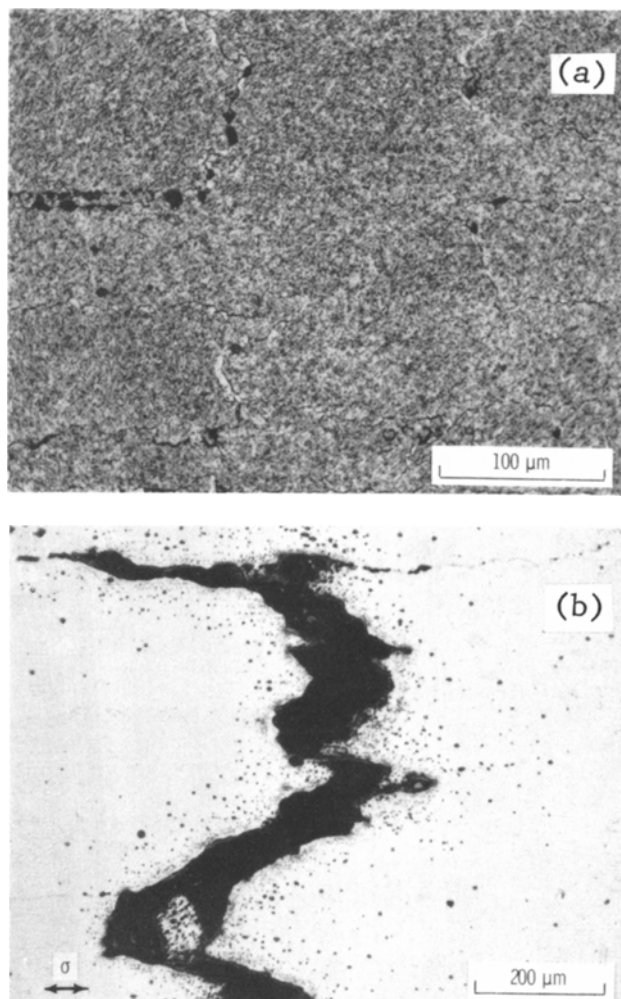


Fig. 3—Typical microstructures of creep-rupture tested ODS alloys. (a) Dispersoid-free bands in Inconel MA-754; 1365 K—82.7 MPa—100.4 h; electrolytically stain etched with chromic acid mixture (100 ml H<sub>2</sub>O, 10 ml H<sub>2</sub>SO<sub>4</sub>, 2 g chromic acid) at 3 to 5 V. (b) Cracking and internal oxidation in TD-NiCrAl; 1365 K—62 MPa—90.0 h—multiple fracture; electrolytically etched with buffered aqua regia (two parts by volume aqua regia, one part glycerine) at 3 to 5 V.

features are not uniformly distributed throughout the gage section; in fact, the bulk of the microstructure is identical to that of as-received (untested) alloy. In essence, the microstructure of tested specimens of DS-NiCr tested in the long transverse direction, Inconel MA-754, TD-NiCrAl, and DST-NiCrAl indicates that creep (or at least that part due to diffusional creep mechanisms) is not homogeneous. Similar behavior has been observed in creep and stress rupture tested TD-NiCr sheet.<sup>16</sup> Additionally Lund and Nix<sup>18</sup> after studying creep in Ni-20Cr-2ThO<sub>2</sub> single crystals concluded that creep in polycrystalline ODS alloys is probably an inhomogeneous process. If creep in polycrystalline alloys is truly inhomogeneous, then correlations between strain rate and stress (for example, Eqs. [1] and [2]) may not be meaningful.

**Threshold Stress.** As previously indicated, it appears that all alloy-direction combinations tested in this study have a threshold stress for creep. For DS-NiCr tested parallel to the extrusion axis, the threshold stress is associated with some type of normal dislocation motion or generation, since DS-NiCr tested parallel to the extrusion axis is essentially a perfect single crystal (no transverse boundaries). Recently Lund and Nix<sup>18</sup> have reported creep test results for single crystal Ni-20Cr-2ThO<sub>2</sub> (TD-NiCr) produced by directional recrystallization; they also found an apparent threshold stress for creep and suggest that it is the Orowan Stress. At 1365 K their threshold stress is about 79 MPa which agrees well with the 69 MPa measured for DS-NiCr in this study, especially since previous work<sup>21</sup> has shown DS-NiCr to be consistently weaker than TD-NiCr.

With the exception of DS-NiCr tested parallel to the extrusion axis, all the ODS alloys tested in this study possessed transverse boundaries in the test section. Thus, these alloys are capable of undergoing slow strain rate plastic deformation by diffusional creep mechanisms in addition to dislocation mechanisms. As shown in Ref. 20, the stress required to produce a strain rate of  $2.78 \times 10^{-8} \text{ s}^{-1}$  (1 pct creep in 100 h) by diffusional creep at 1365 K for a 250 μm grain size ODS Ni alloy is about 17 MPa. Both Inconel MA-754 and TD-NiCrAl have approximately a 250 μm grain size; and, as can be seen in Table V, both alloys require stress levels in excess of 17 MPa in order to produce a strain rate of  $2.8 \times 10^{-8} \text{ s}^{-1}$ . Thus, diffusional creep mechanisms alone can produce more deformation than is observed. These calculations and the microstructural evidence of diffusional creep (dispersoid-free bands) in large grain size ODS alloys support the concept that the threshold stress is associated with diffusional creep rather than dislocation creep mechanisms.

Explanation of the threshold stress in TD-Ni is more difficult than those for single crystalline or large grain size alloys. It is tempting to also ascribe this threshold stress to diffusional creep; however, because of the very small grain size in TD-Ni, exceeding the threshold stress by moderate amounts should result in extremely high diffusional creep rates. For example, at 1365 K,  $(\sigma - \sigma_0) = 1 \text{ MPa}$  would mean a steady state diffusional creep rate of about  $10^{-4} \text{ s}^{-1}$ . Accounting for the high grain aspect ratio of TD-Ni would lower these creep rates; how-

ever, Raj and Ashby<sup>15</sup> estimate that the rate would only be reduced by the square root of the grain aspect ratio ( $\sqrt{19}$  for TD-Ni). Either creep in TD-Ni is not controlled by diffusional mechanisms, or perhaps the measured threshold stress is at the lower end of a range of threshold stresses. Such a range could account for inhomogeneous deformation resulting in the low strain rates.

The threshold stress seems to be associated with diffusional creep in the large grain size ODS alloys: Inconel MA-754, TD-NiCrAl, and DST-NiCrAl. Comparison of the threshold stress values in Table VI to the grain size parameters in Table III indicates that no apparent relationship between threshold stress and grain size exists. There does, however, appear to be a linear relationship between 1365 K threshold stresses and grain aspect ratio as shown in Fig. 4. Included in this figure are the threshold stress data for thin TD-NiCr sheet;<sup>17</sup> the pertinent data for this material are presented in Table VII. The curve shown in Fig. 4 is described by

$$\sigma_0 = 6 + 18.1 (\text{GAR}) \quad [3]$$

where  $\sigma_0$  is in MPa and GAR is the grain aspect ratio reported in Tables III and VII. This figure indicates that the threshold stress for creep in polycrystalline alloys is dependent on the ratio of grain boundary area in shear to grain boundary area in tension. While Eq. [3] accurately describes the relationship between threshold stress and grain aspect ratio for thick material, as can be seen in Table VII, Eq. [3] overestimates the threshold stress when very thin material is under consideration. However, as the 0.025 cm thick TD-NiCr sheet was consistently weaker than the 0.051 cm sheet,<sup>17</sup> it is not surprising that the

0.025 cm thick sheet did not show results consistent with Eq. [3]. Apparently 0.025 cm thick TD-NiCr sheet is not representative of bulk material.

Overall it appears that the threshold stresses for ODS Ni-20Cr and Ni-16Cr-4/5Al type alloys are uniquely dependent on the grain aspect ratio. For such alloys with grain sizes between 150 and 400  $\mu\text{m}$  and grain aspect ratios between 0.8 and 3.5, threshold stresses at 1365 K can be calculated from Eq. [3] with, apparently, good accuracy. Use of Eq. [3] beyond the stated grain size and grain aspect ratio limits is not recommended without supporting experimental data. For instance, at sufficiently high grain aspect ratios, the predicted threshold stress would exceed the stress required for dislocation motion (Orowan stress).

As shown elsewhere,<sup>17,20</sup> the residual room temperature tensile properties of large grain size ODS alloys are greatly affected by prior elevated temperature creep. For example, prior creep strains as low as 0.2 pct can reduce the tensile ductility as much as 50 pct. Such behavior seemingly limits the use of large grain size ODS alloys to conditions where creep does not occur. Thus, threshold stress may be the most important creep strength property for these alloys. For use of these particular alloys, the threshold stress is recommended as the base design criteria rather than more conventional use of a stress to produce a known amount of creep in finite time.

- INCONEL MA-754: PARALLEL EXTRUSION AXIS
- INCONEL MA-754: LONG TRANSVERSE
- ◇ TD-NiCrAl: PARALLEL EXTRUSION AXIS
- △ DST-NiCrAl: PARALLEL EXTRUSION AXIS
- TD-NiCr, HEAT 3636: PARALLEL ROLLING DIRECTION (ESTIMATED)
- ◇ TD-NiCr, HEAT 3636: NORMAL ROLLING DIRECTION
- △ TD-NiCr, HEAT 3712: PARALLEL ROLLING DIRECTION
- ▽ TD-NiCr, HEAT 3712: NORMAL ROLLING DIRECTION

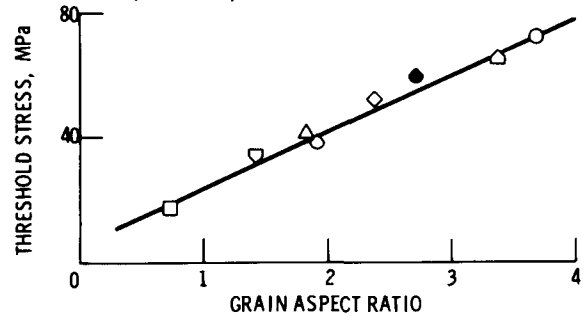


Fig. 4—1365 K threshold stresses for various large grain size ODS alloys as a function of grain aspect ratio.

Table VI. 1365 K Stress Exponents and Estimated Threshold Stresses for ODS Alloys

Alloy	Direction	Stress Exponent	Threshold Stress, MPa	Effective Stress Exponent
TD-Ni	Parallel to ext axis	13.5	53	2.4
Inconel MA-754	Parallel to ext axis	18	72	1
Inconel MA-754	Long transverse	16	17	1.4
DS-NiCr	Parallel to ext axis	41	69	9
DS-NiCr	Long transverse	*	55	*
TD-NiCrAl	Parallel to ext axis	23	52	*
DST-NiCrAl	Parallel to ext axis	10.5	41	1

\*Could not be determined

Table VII. Grain Size Parameters and Threshold Stress for Thin TD-NiCr (Ni-20Cr-2ThO<sub>2</sub>) Sheet (Ref. 17)

Heat	Orientation is Reference to Sheet Rolling Direction	Characteristic Length, $\mu\text{m}$		Sheet Thickness Direction, $L_3$	Grain Size, $\mu\text{m}$ $0.85 \sqrt[3]{L_1 L_2 L_3}$	Grain Aspect Ratio, GAR $L_1 / \sqrt{L_2 L_3}$	Threshold Stress, MPa	
		Parallel to Test Direction, $L_1$	Perpendicular to Test Direction, $L_2$				Measured	Calculated Eq. [3]
3636	Parallel	290	230	50	150	2.7	59*	55.0
(0.051 cm thick)	Normal	230	290	50	150	1.9	38	40.5
3712	Parallel	640	360	100	240	3.37	65	67.0
(0.051 cm thick)	Normal	360	640	100	240	1.42	34	31.7
3637	Parallel	390	290	53	165	3.15	45	63.0
(0.025 cm thick)	Normal	290	390	53	165	2.0	32	42.2

\*Estimated.



Finally, it should be noted that the threshold stresses estimated in this work are based on the results of nominally 100 h creep tests at 1365 K. It has previously been shown<sup>17,18</sup> that threshold stresses are dependent on temperature; in addition, threshold stresses may be dependent on time. As one conducts longer creep tests (>100 h), the ability to measure lower creep rates ( $<10^{-9} \text{ s}^{-1}$ ) is increased. Thus, threshold stresses estimated from creep curves may be reduced since one is better able to detect very small strain rates.

### CONCLUSIONS

Based on a study of tensile creep at 1365 K of several ODS Ni-base alloys the following conclusions are drawn:

- 1) ODS alloys possess threshold stresses for creep.
- 2) Creep in polycrystalline ODS alloys is an inhomogeneous process.
- 3) The threshold stresses in large grain size ODS Ni-20Cr and Ni-16Cr-4/5Al type alloys are dependent on the grain aspect ratio.
- 4) Maximum design criteria for large grain size ODS alloys should be limited to the threshold stress for creep.

### REFERENCES

1. G. S. Doble and R. J. Quigg *Trans. TMS-AIME*, vol. 233, 1965, pp. 410-15.
2. B. A. Wilcox and A. H. Clauer *Trans. TMS-AIME*, vol. 236, 1966, pp. 570-80.
3. C. E. Lowell, S. J. Grisaffe, and D. L. Deadmore *Ox. Metals*, vol. 4, no. 2, 1972, pp. 91-111.
4. B. A. Wilcox, A. H. Clauer, and W. S. McCam *Trans. TMS-AIME*, vol. 239, 1967, pp. 1791-95.
5. L. J. Fritz, W. P. Koster, and R. E. Taylor NASA CR-121221, 1973.
6. C. E. Lowell, D. L. Deadmore, S. J. Grisaffe, and I. L. Drell: NASA TN D-6290, 1971.
7. J. R. Johnston and R. L. Ashbrook NASA TN D-5376, 1969.
8. C. E. Lowell and W. A. Sanders *Ox. Metals*, vol. 5, no. 3, 1972, pp. 221-39.
9. L. J. Klingler, W. R. Wemberger, P. G. Bailey, S. Baranow: NASA CR-120796, 1972.
10. D. L. Klarstrom and R. Grierson. NASA CR 134901, 1975.
11. D. L. Deadmore, C. E. Lowell, and G. J. Santoro NASA TM X-71835, 1975.
12. B. A. Wilcox and A. H. Clauer *The Superalloys*, C. T. Sims and W. C. Nagel, eds., p. 197, John Wiley and Sons, 1972.
13. P. G. Bailey *The Sixth National Sampe Technical Conference*, vol. 6, p. 208, SAMPE, Azusa, Calif. 91702.
14. R. D. Kane and L. J. Ebert *Met. Trans. A*, vol. 7A, 1976, pp. 133-37.
15. R. Raj and M. F. Ashby *Met. Trans.*, vol. 2, 1971, pp. 1113-25.
16. J. D. Whittenberger: *Met. Trans.*, vol. 4, 1973, pp. 1475-83.
17. J. D. Whittenberger: *Met. Trans. A*, vol. 7A, 1976, pp. 611-19.
18. R. W. Lund and W. D. Nix: *Acta Met.*, vol. 24, no. 5, 1976, pp. 469-79.
19. J. Lin and O. D. Sherby: Second Annual Report, NASA Grant NGR-05-020-671.
20. J. D. Whittenberger: NASA TN D-8421, 1977.
21. P. G. Bailey and R. E. Kutchea AFML-TR-73-294, 1973.